



Figures and figure supplements

Neuroprotective effects of TRPA1 channels in the cerebral endothelium following ischemic stroke

Paulo Wagner Pires and Scott Earley

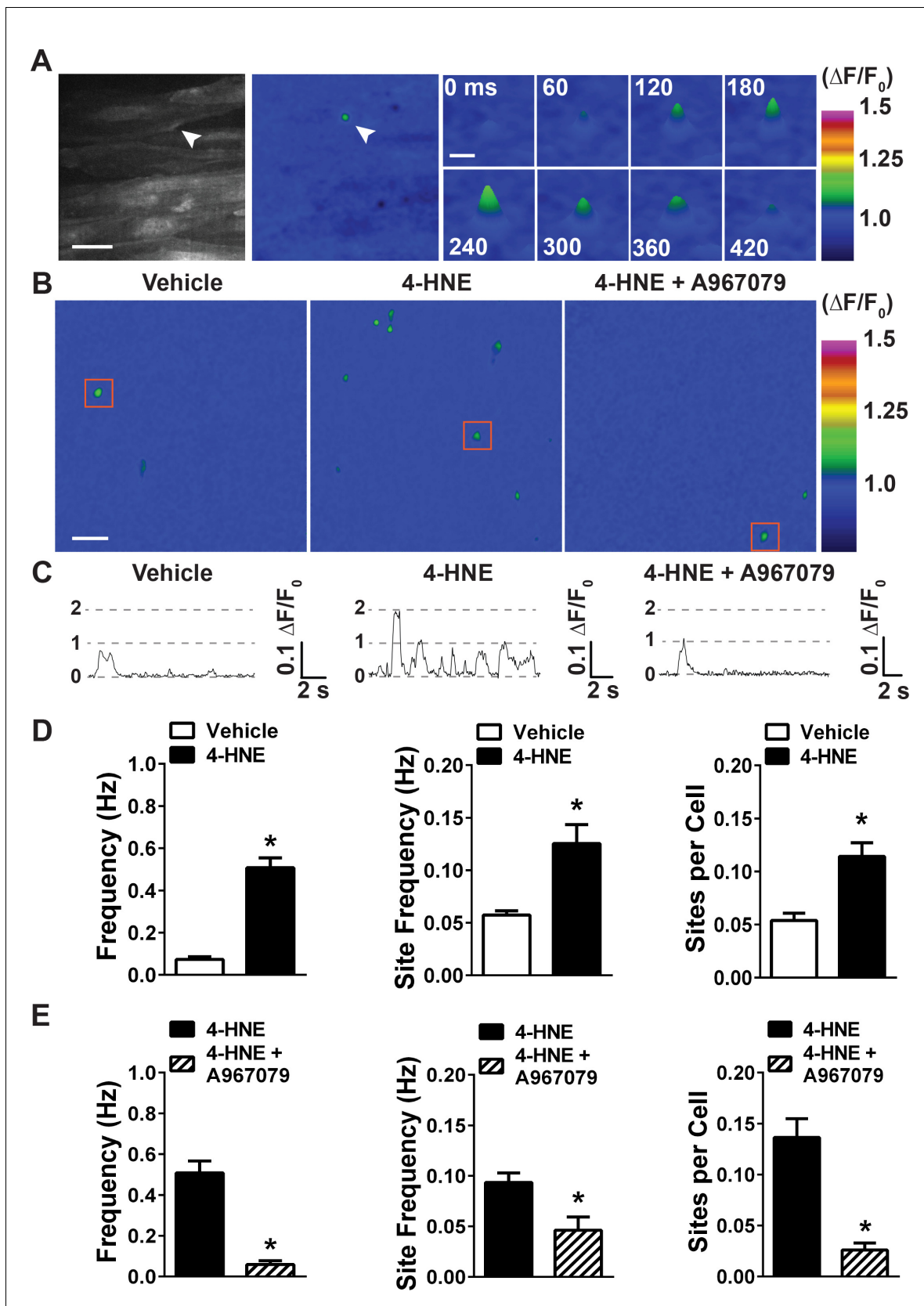


Figure 1. 4-HNE stimulates TRPA1 sparklets in the endothelium of intact cerebral arteries. (A) Representative images of endothelial cells from cerebral arteries from *Tek:Gcamp6f* mice mounted *en face*, presented in grayscale (left) and pseudocolored (middle and right panels). Scale bar = 15 μ m. The Figure 1 continued on next page

Figure 1 continued

images on the right are a timelapse and digital magnification of the TRPA1 sparklet indicated by the arrow in the right and middle panels. Scale bar = 5 μm . (B) Representative pseudocolored images of a 512×512 pixels field of view from *Tek:Gcamp6f* mice showing sparklets (green) after exposure to vehicle, 4-HNE and 4-HNE + A967079. Scale bar = 20 μm . (C) Representative $\Delta F/F_0$ vs. time plots for a single sparklet site. 0, 1, two levels indicate hypothesized numbers of TRPA1 channels engaged during each signal. (D) Summary data showing the effects of the TRPA1 channel activator 4-HNE (1 μM) on TRPA1 sparklet frequency, site frequency and number of sites per cell ($n = 24$ fields of view from four different arteries, $N = 4$ mice). (E) TRPA1 inhibition with A967079 (1 μM) significantly prevented 4-HNE induction of TRPA1 sparklets in endothelial cells (20 fields of view from five different arteries; $N = 3$ mice). Data are presented as means \pm SEM (* $p < 0.05$, Student's t-test). TRPA1 sparklets were recorded in the presence of the cell permeable Ca^{2+} chelator EGTA-AM (10 μM) and the sarcoendoplasmic reticulum Ca^{2+} -ATPase inhibitor cyclopiazonic acid (CPA, 30 μM).

DOI: <https://doi.org/10.7554/eLife.35316.003>

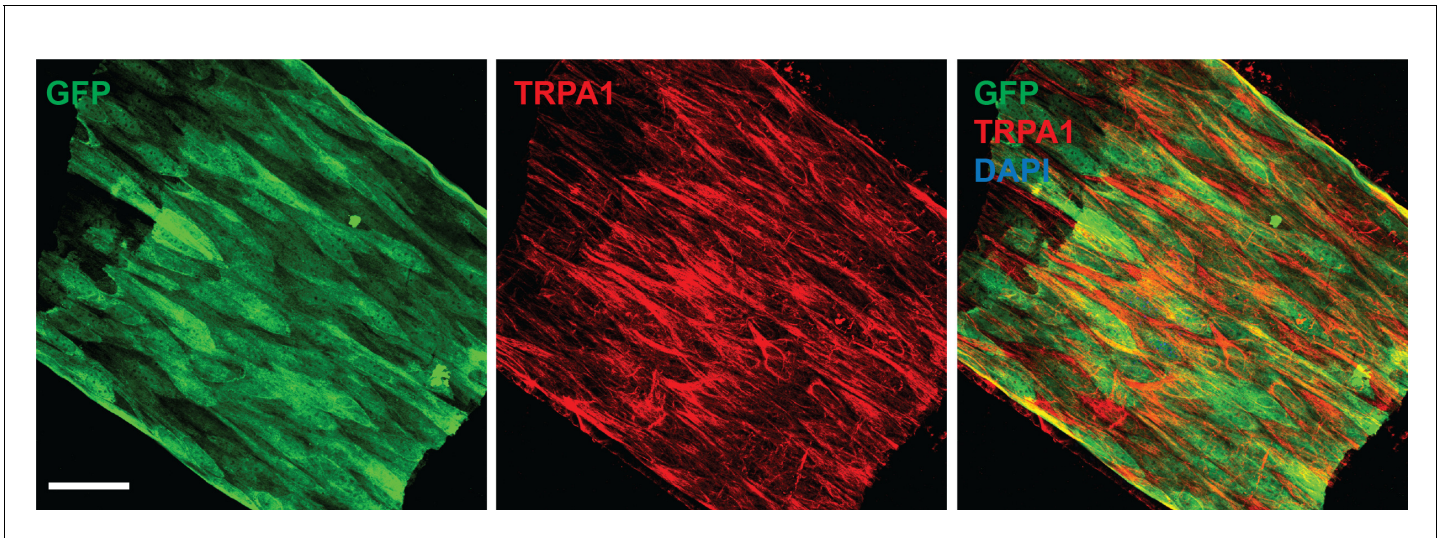


Figure 1—figure supplement 1. TRPA1 is present in the endothelium of cerebral arteries. (A) Representative maximum intensity projection laser scanning confocal images showing immunolabeling of TRPA1 channels (red) in EGFP-expressing endothelial cells (green) of a pial artery in the brain of a perfusion-fixed *Tek^{EGFP}* mouse. Nuclei of cells were stained by DAPI (blue). Scale bar = 40 μ m.

DOI: <https://doi.org/10.7554/eLife.35316.004>

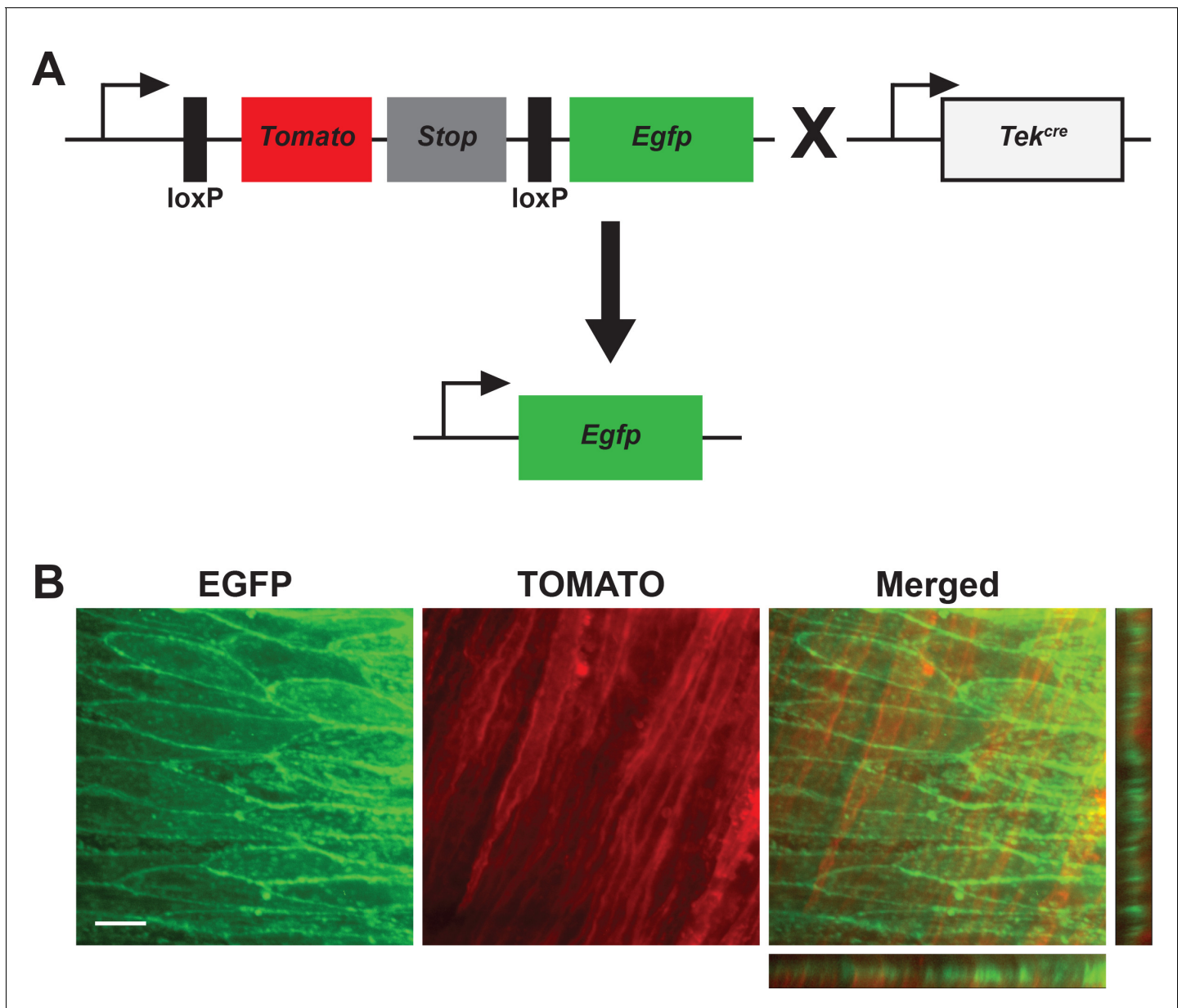


Figure 1—figure supplement 2. Reporter expression of *cre*-recombinase using the *mT/mG* reporter mice. (A) Diagram of the genetic construct of the *mT/mG* reporter mice. Upon crossing with a mouse line expressing *cre*-recombinase, the sequence for *Tomato* and the *Stop* codon are excised, and *Egfp* is expressed. (B) Representative image of an *en face* cerebral artery from *Tek:mT/mG* showing EGFP expression (green) in the endothelial cell layer and TOMATO (red) in the underlying smooth muscle layer. The orthogonal sections on the right show that there is no overlap between green and red fluorescence. Scale bar = 20 μ m.

DOI: <https://doi.org/10.7554/eLife.35316.005>

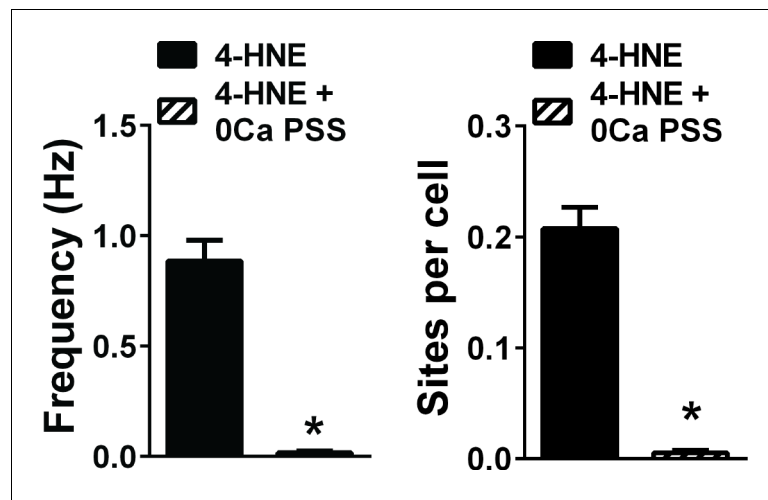


Figure 1—figure supplement 3. Extracellular Ca^{2+} is required for TRPA1 sparklets. Removal of extracellular Ca^{2+} significantly reduces TRPA1 sparklet frequency and number of sparklet sites induced by 4-HNE. * $p < 0.05$, Student's t-test. $n = 36$ fields of view from three different *Tek:Gcamp6f* mice. TRPA1 sparklets were recorded in the presence of the cell permeable Ca^{2+} chelator EGTA-AM (10 μM) and the sarcoendoplasmic reticulum Ca^{2+} -ATPase inhibitor cyclopiazonic acid (CPA, 30 μM).

DOI: <https://doi.org/10.7554/eLife.35316.006>

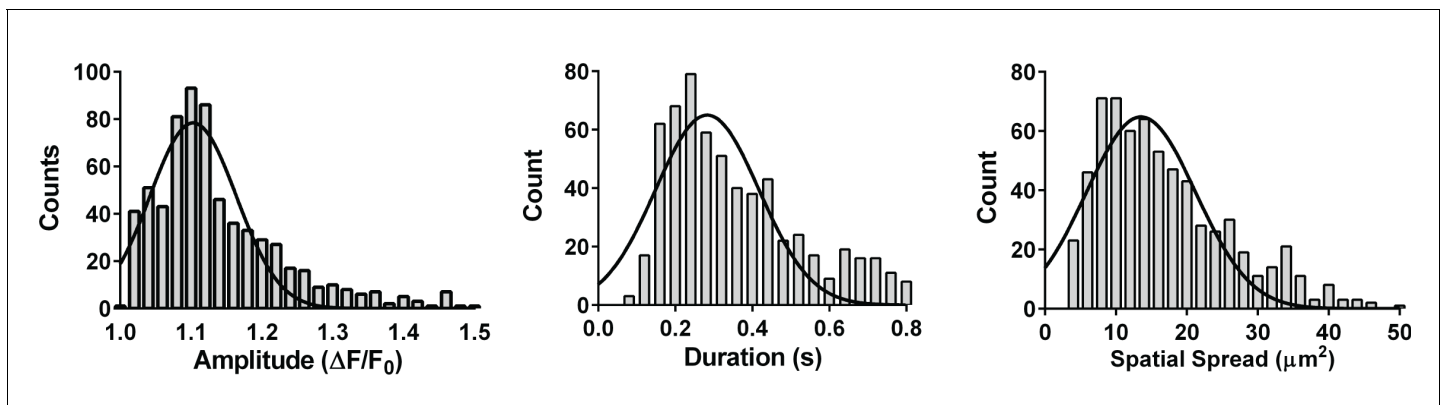


Figure 1—figure supplement 4. Properties of 4-HNE-induced TRPA1 sparklets. Frequency distribution plots of 4-hydroxynonenal (4-HNE)-induced TRPA1 sparklets in *en face* cerebral arteries from *Tek:Gcamp6f* mice. Recorded events showed a mode amplitude of $1.10 \Delta F/F_0$, a mode duration of 240 ms and a mode spatial spread of $10 \mu m^2$. A total of 670 events were plotted to analyze frequency distribution. TRPA1 sparklets were recorded in the presence EGTA-AM ($10 \mu M$) and CPA ($30 \mu M$).

DOI: <https://doi.org/10.7554/eLife.35316.008>

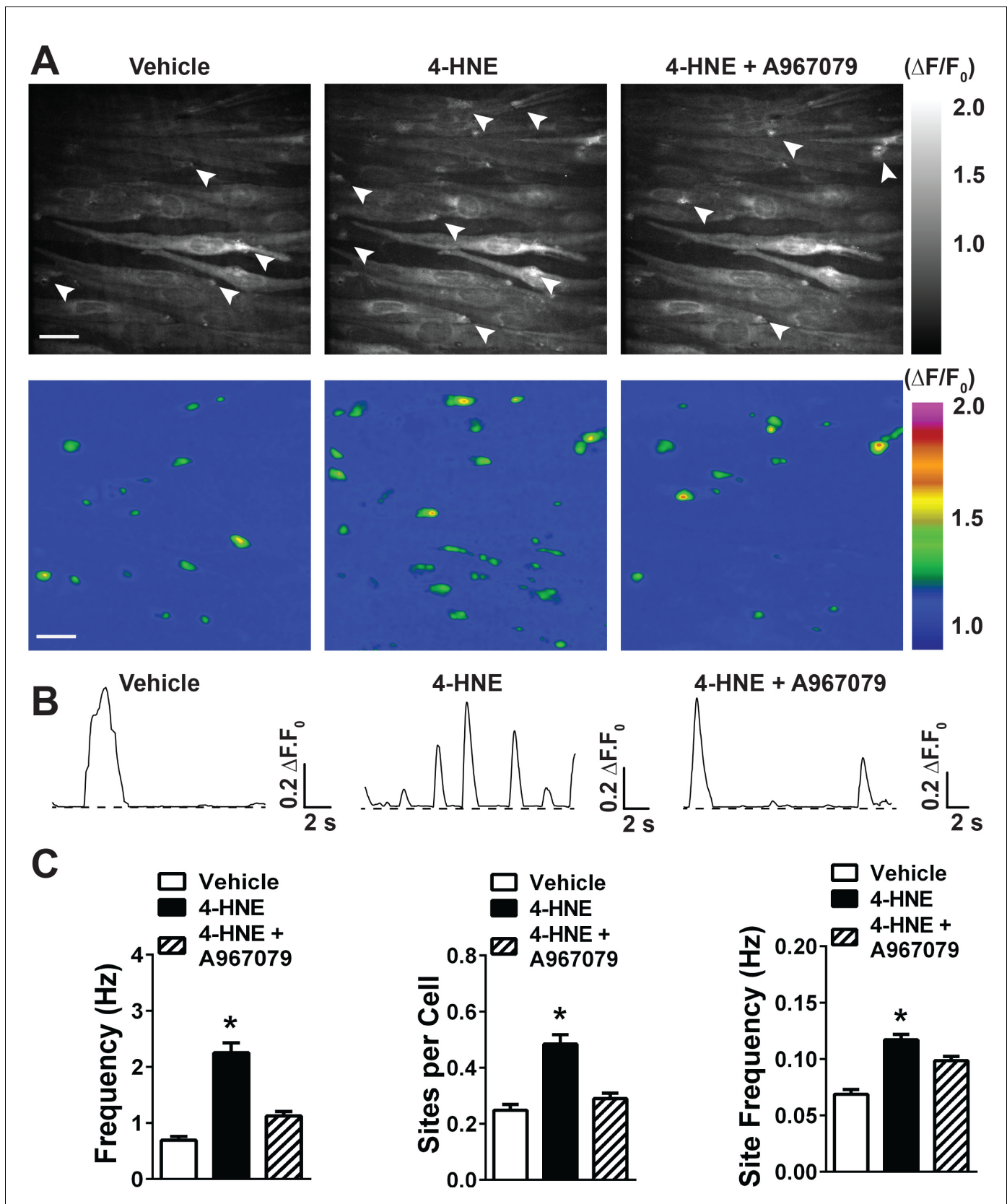


Figure 2. 4-HNE stimulates large Ca^{2+} transients in the endothelium of intact cerebral arteries. (A) Representative grayscale images of endothelial cells from *Tek:Gcamp6f* mice mounted *en face* in the absence of CPA and EGTA-AM. The white arrowheads point to sites of Ca^{2+} transients. Scale bar = 30 μm . Figure 2 continued on next page

Figure 2 continued

μm . Pseudocolored representations of the images are shown below. Scale bar = 30 μm . **(B)** Representative $\Delta F/F_0$ vs. time plots of Ca^{2+} transients from a single site of Ca^{2+} transients. **(C)** Summary graphs showing that 4-HNE (1 μM) significantly increases frequency, number of active sites, and site frequency of Ca^{2+} transients in cerebral artery endothelial cells. This response was diminished by the TRPA1 blocker A967079 (1 μM). (25 fields of view from three different arteries; N = 3 mice). Data are presented as means \pm SEM (* $p < 0.05$, one-way ANOVA).

DOI: <https://doi.org/10.7554/eLife.35316.017>

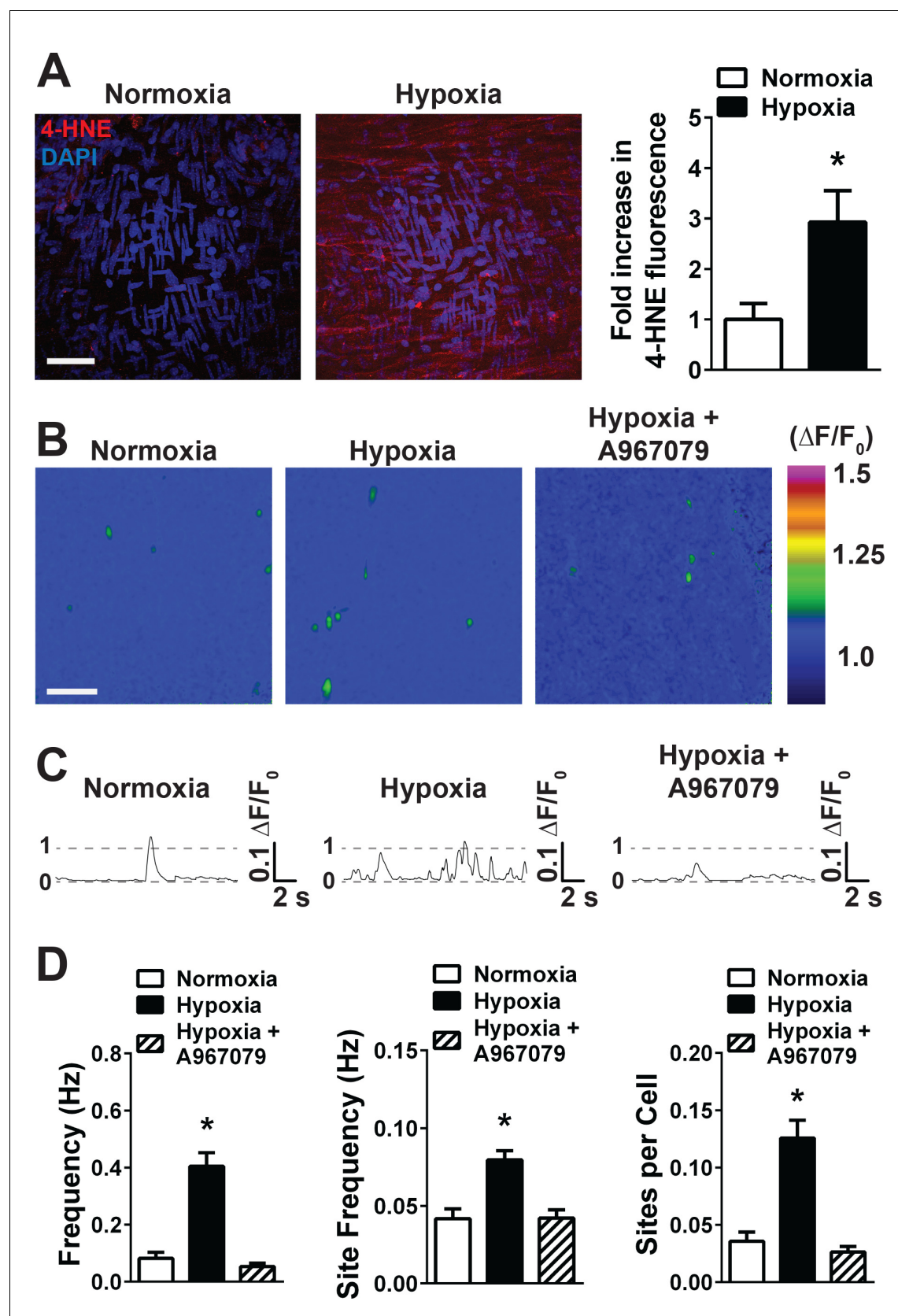


Figure 3. Acute hypoxia increases 4-HNE accumulation and increases TRPA1 sparklet frequency in the cerebral endothelium. (A) Representative maximum intensity projection of Z-stacks of cerebral arteries mounted *en face* and exposed to PSS equilibrated with a normoxic (21% O₂, 6% CO₂, 73% N₂) atmosphere. (B) Representative maximum intensity projection of Z-stacks of cerebral arteries mounted *en face* and exposed to PSS equilibrated with a hypoxic (1% O₂, 6% CO₂, 93% N₂) atmosphere. (C) Representative traces of TRPA1 sparklet frequency (normalized to $\Delta F/F_0$) over time (2 s). (D) Bar graphs of TRPA1 sparklet frequency (Hz), site frequency (Hz), and sites per cell for Normoxia, Hypoxia, and Hypoxia + A967079. * indicates statistical significance.

Figure 3 continued on next page

Figure 3 continued

N₂, left panel) or hypoxic gas mixture (5% O₂, 6% CO₂, 89% N₂, right panel) and immunolabeled for 4-HNE (red). Scale bar = 40 μ m, nuclei of cells are labeled by DAPI (blue). Acute hypoxia significantly increased 4-HNE immunoreactivity in cerebral arteries (* p <0.05 *Student's t*-test, N = 10–9 fields of view from three different experiments). (B) Representative pseudocolored images of cerebral arteries from *Tek:Gcamp6f* mice mounted *en face* and exposed to normoxic (left panel) or hypoxic (middle and right panels) PSS in the presence or absence of the selective TRPA1 blocker A967079 (1 μ M). Green: active TRPA1 sparklet sites. Scale bar = 20 μ m. (C) Representative $\Delta F/F_0$ vs. time plots for a single sparklet site showing an increase in TRPA1 sparklet frequency during hypoxia which was significantly inhibited by the TRPA1 blocker A967079. (D) Summary data showing the effects of hypoxia on TRPA1 sparklet frequency (left), site frequency (middle) and number of sites per cell (right) in the presence and absence of the selective TRPA1 inhibitor A967079 (1 μ M). (* p <0.05, one-way ANOVA; N = 25–28 – 33 fields of view from six different arteries isolated from six mice). TRPA1 sparklets were recorded in the presence EGTA-AM (10 μ M) and CPA (30 μ M).

DOI: <https://doi.org/10.7554/eLife.35316.022>

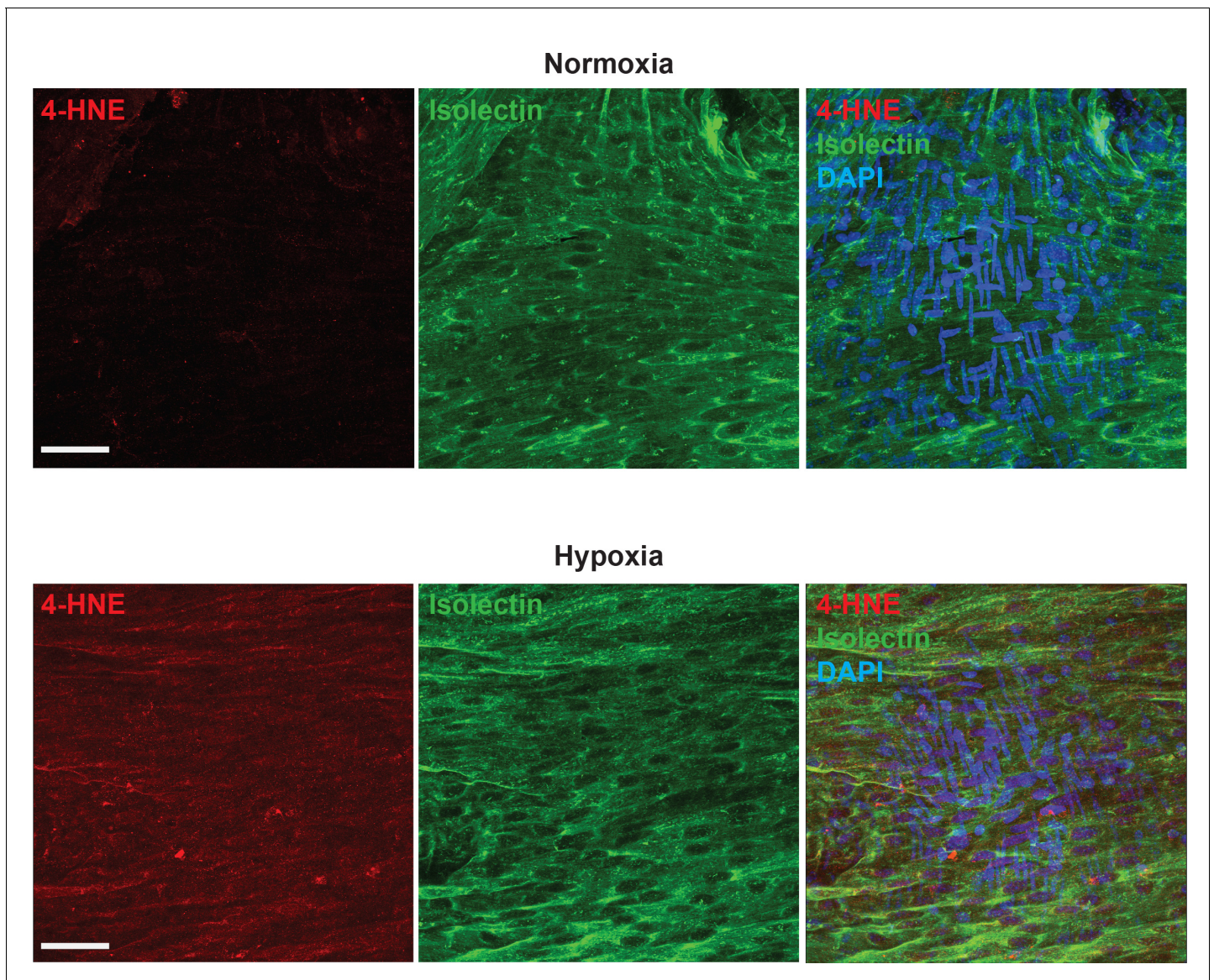


Figure 3—figure supplement 1. Hypoxia causes 4-HNE accumulation in cerebral arteries. Representative maximum intensity projection images of *en face* cerebral arteries immunolabeled for 4-HNE (red) and stained with isolectin conjugated to AlexaFluor 488 (green) after superfused with normoxic (top images) or hypoxic (bottom panels) physiological saline solution (PSS). The panels on the right are overlay images showing nuclei staining (DAPI, blue). Images are representative of 3 different experiments from 10 basilar arteries. Scale bar = 40 μ m.

DOI: <https://doi.org/10.7554/eLife.35316.023>

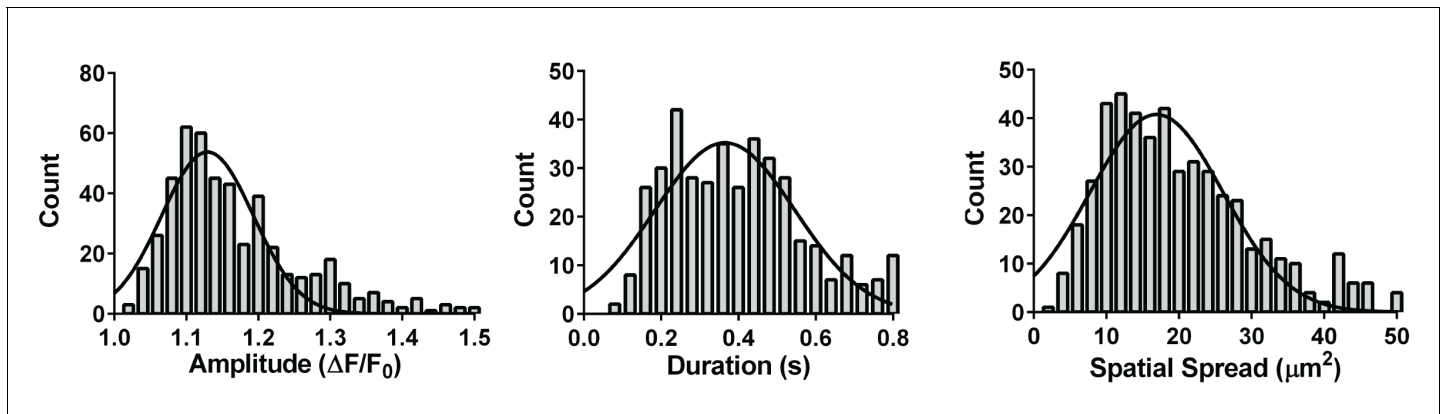


Figure 3—figure supplement 2. Properties of hypoxia-induced TRPA1 sparklets. Frequency distribution plots of hypoxia-induced TRPA1 sparklet in *en face* cerebral arteries from *Tek:Gcamp6f* mice. Recorded events showed a mode peak amplitude of $1.10 \Delta F/F_0$, a mode duration of 240 ms and a mode spatial spread of $12 \mu m^2$. A total of 437 events were plotted to analyze frequency distribution. TRPA1 sparklets were recorded in the presence of EGTA-AM ($10 \mu M$) and CPA ($30 \mu M$).

DOI: <https://doi.org/10.7554/eLife.35316.025>

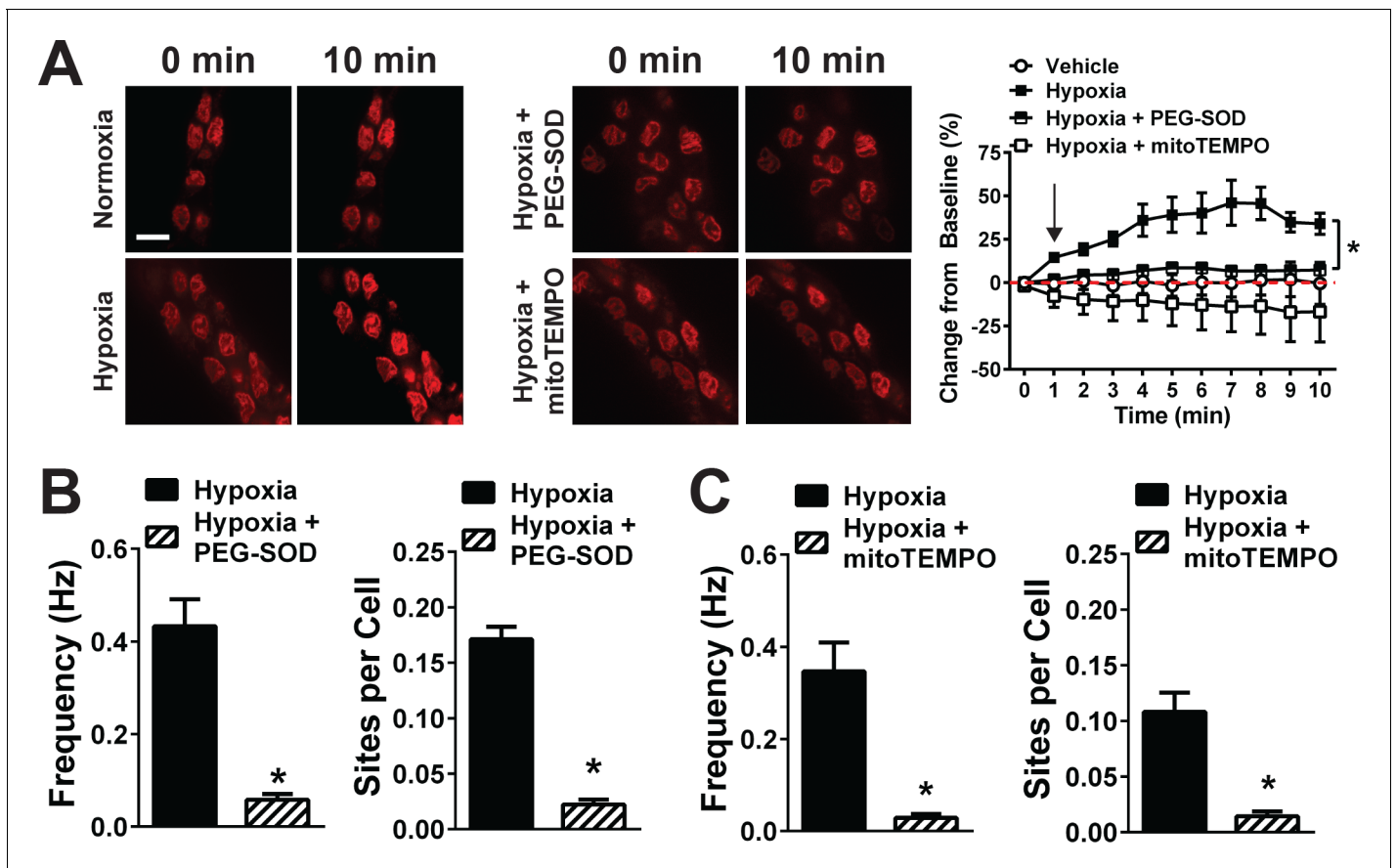


Figure 4. Acute hypoxia induces mitochondrial superoxide generation and increases TRPA1 sparklet frequency in the cerebral endothelium. (A) *Left and middle:* Superoxide generation detected with the superoxide-sensitive dye DHE (red) in the endothelium of cerebral arteries mounted *en face* under normoxia (left), hypoxia (left), hypoxia plus the membrane-permeable PEG-SOD (100 U/ml, middle) and hypoxia plus the mitochondria-targeted SOD mimetic mitoTEMPO (500 nM, middle). *Right:* Summary data showing changes in DHE fluorescence over time under each condition (* $p < 0.05$, two-way ANOVA; $n = 5-7-6-7$ arteries from five different mice). The arrow in the graph indicates the onset of hypoxia. Scale bar = 10 μm . (B and C) Summary data showing the effects of PEG-SOD (B) and mitoTEMPO (C) on the frequency and number of active TRPA1 sparklet sites in the cerebral artery endothelium of *Tek:Gcamp6f* mice (* $p < 0.05$, Student's *t*-test; $n = 25-30$ fields of view from six different preparations isolated from six different mice). TRPA1 sparklets were recorded in the presence of EGTA-AM (10 μM) and (CPA, 30 μM).

DOI: <https://doi.org/10.7554/eLife.35316.030>

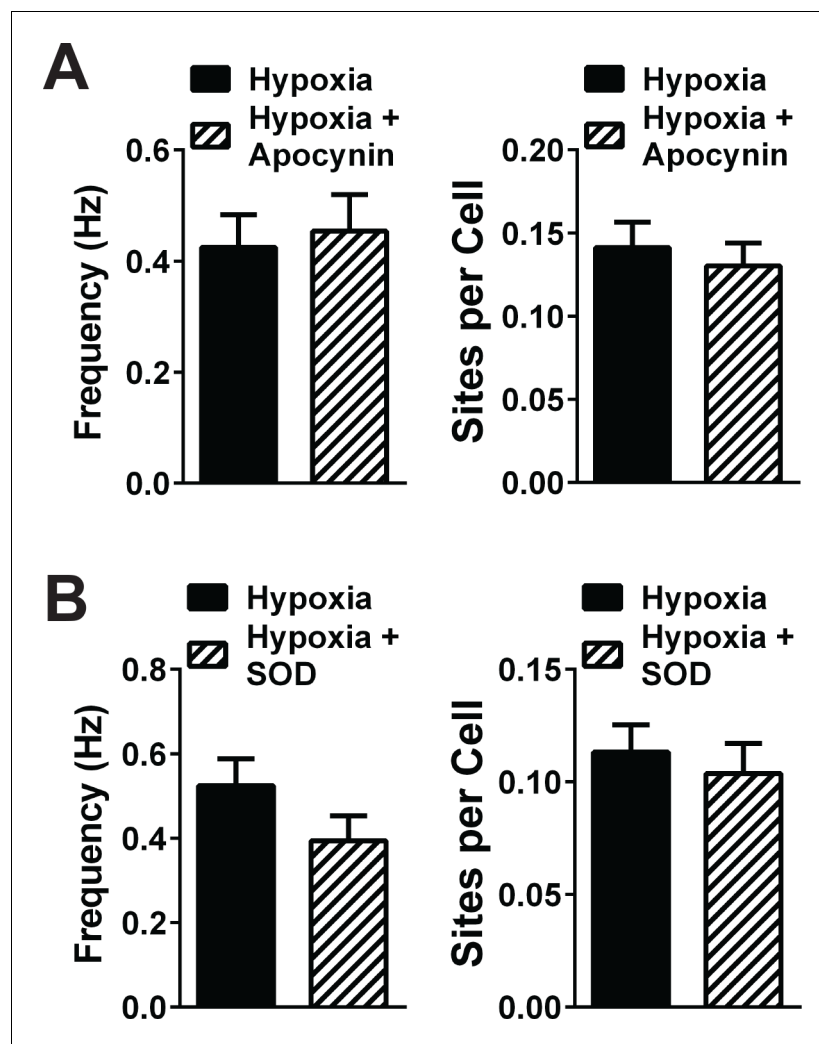


Figure 4—figure supplement 1. NOX2 inhibition and extracellular SOD did not significantly inhibit hypoxia-induced TRPA1 sparklets. (A) Summary graph showing that sparklet frequency and number of TRPA1 sparklet sites induced by hypoxia are not significantly changed by apocynin. N = 25–30 fields of view from three different *Tek:Gcamp6f* mice. (B) Summary graph showing that TRPA1 sparklet frequency and number of sparklet sites induced by hypoxia are not significantly altered by incubation with extracellular SOD. N = 25–30 fields of view from three different *Tek:Gcamp6f* mice. TRPA1 sparklets were recorded in the presence of EGTA-AM (10 μ M) and CPA (30 μ M).

DOI: <https://doi.org/10.7554/eLife.35316.031>

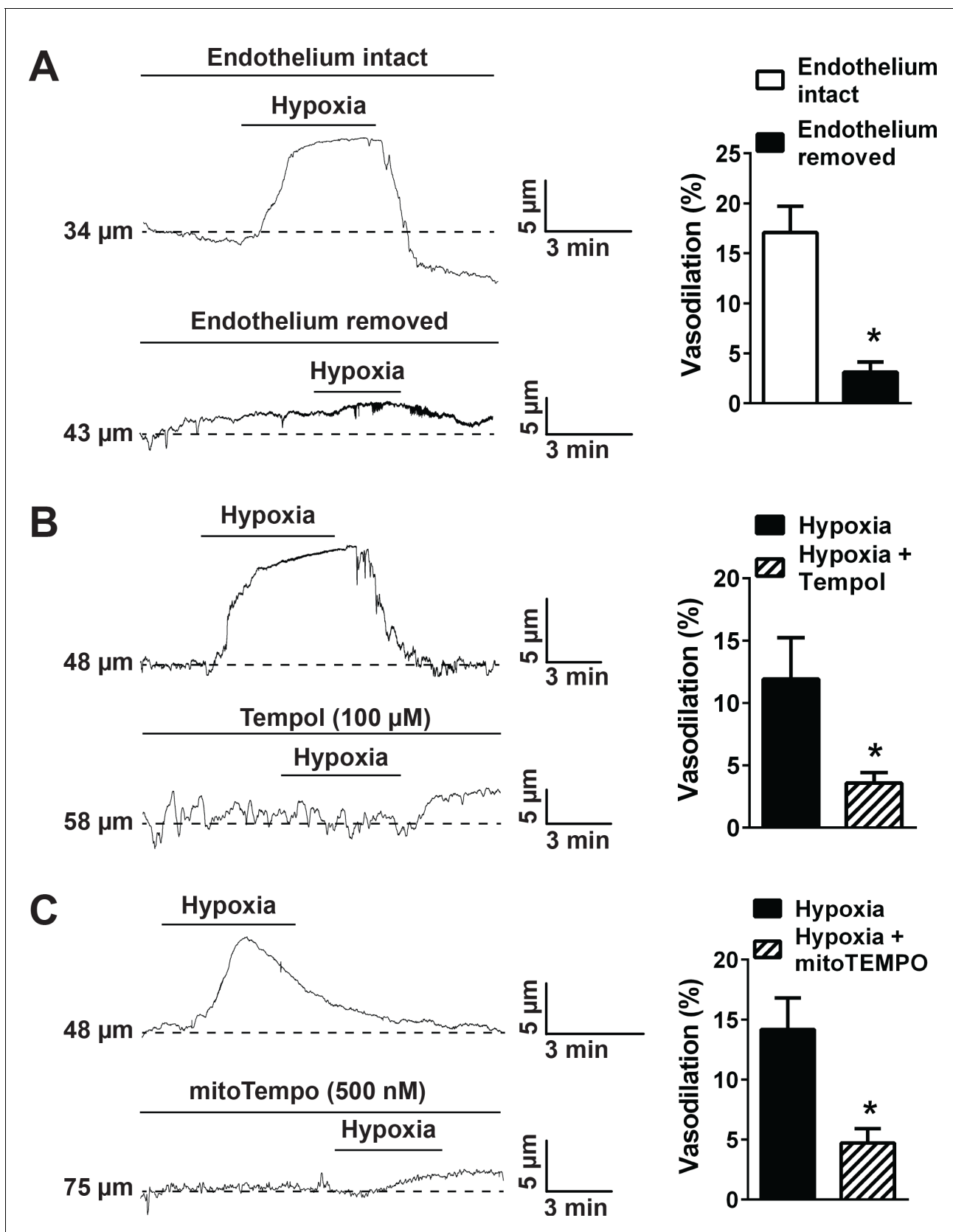


Figure 5. Hypoxia acts via mitochondrial superoxide to induce endothelium-dependent dilation of pressurized cerebral arteries. (A) Representative traces (left) and summary data (right) showing hypoxia-induced dilation in intact and endothelium-denuded cerebral pial arteries (* $p < 0.05$, Student's t -test). Figure 5 continued on next page

Figure 5 continued

test; $n = 5$ arteries from three different mice). (B) Representative traces of lumen diameter of a pressurized cerebral pial artery (left) and summary data (right) showing hypoxia-induced dilation in the presence of the cell-permeant SOD mimetic Tempol ($100 \mu\text{M}$). (* $p < 0.05$, Student's t-test; $n = 5$ arteries from three different mice.) (C) Representative traces of the lumen diameter of a pressurized cerebral pial artery (left) and summary data (right) showing hypoxia-induced dilation in the presence of the cell-permeant mitochondrial membrane-targeted SOD mimetic mitoTEMPO (500 nM). (* $p < 0.05$, Student's t-test; $n = 6$ arteries from three different mice). The arteries used for pressure myography experiments were not treated with EGTA-AM or CPA.

DOI: <https://doi.org/10.7554/eLife.35316.034>

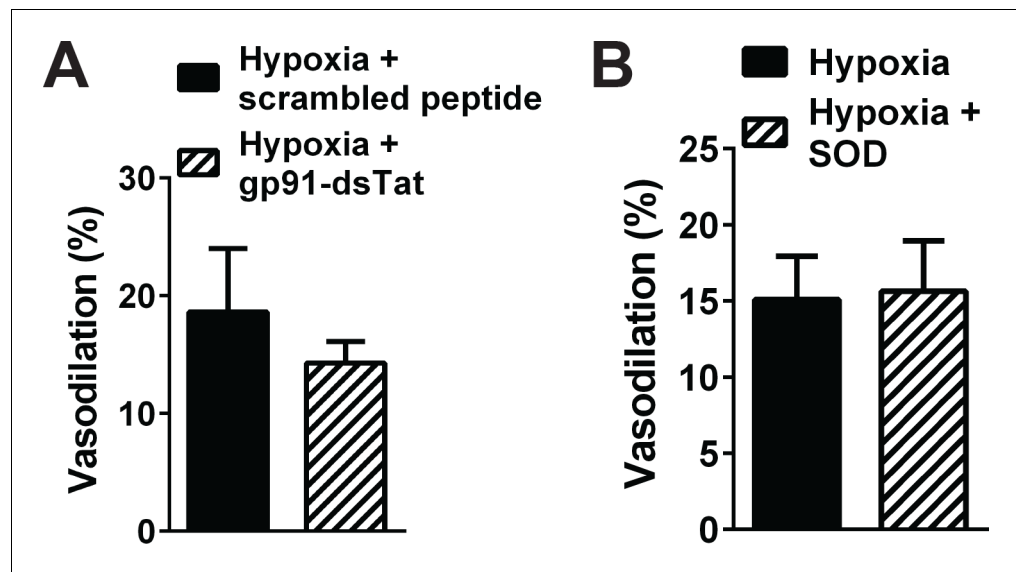


Figure 5—figure supplement 1. NOX2 inhibition and quenching of extracellular O_2^- and H_2O_2 did not significantly alter cerebral artery dilation induced by hypoxia. Summary data showing that hypoxia-induced dilation of cerebral pial arteries was not significantly altered by NOX2 inhibition with gp91-dsTat (1 μ M, (A), and by removal of extracellular O_2^- with SOD (200 U/mL, (B). $n = 3$ arteries from three different mice for the gp91-dsTat experiments, and $n = 5$ arteries from three different mice for the extracellular SOD experiments. Arteries used for pressure myography experiments were not incubated with EGTA-AM or CPA.

DOI: <https://doi.org/10.7554/eLife.35316.035>

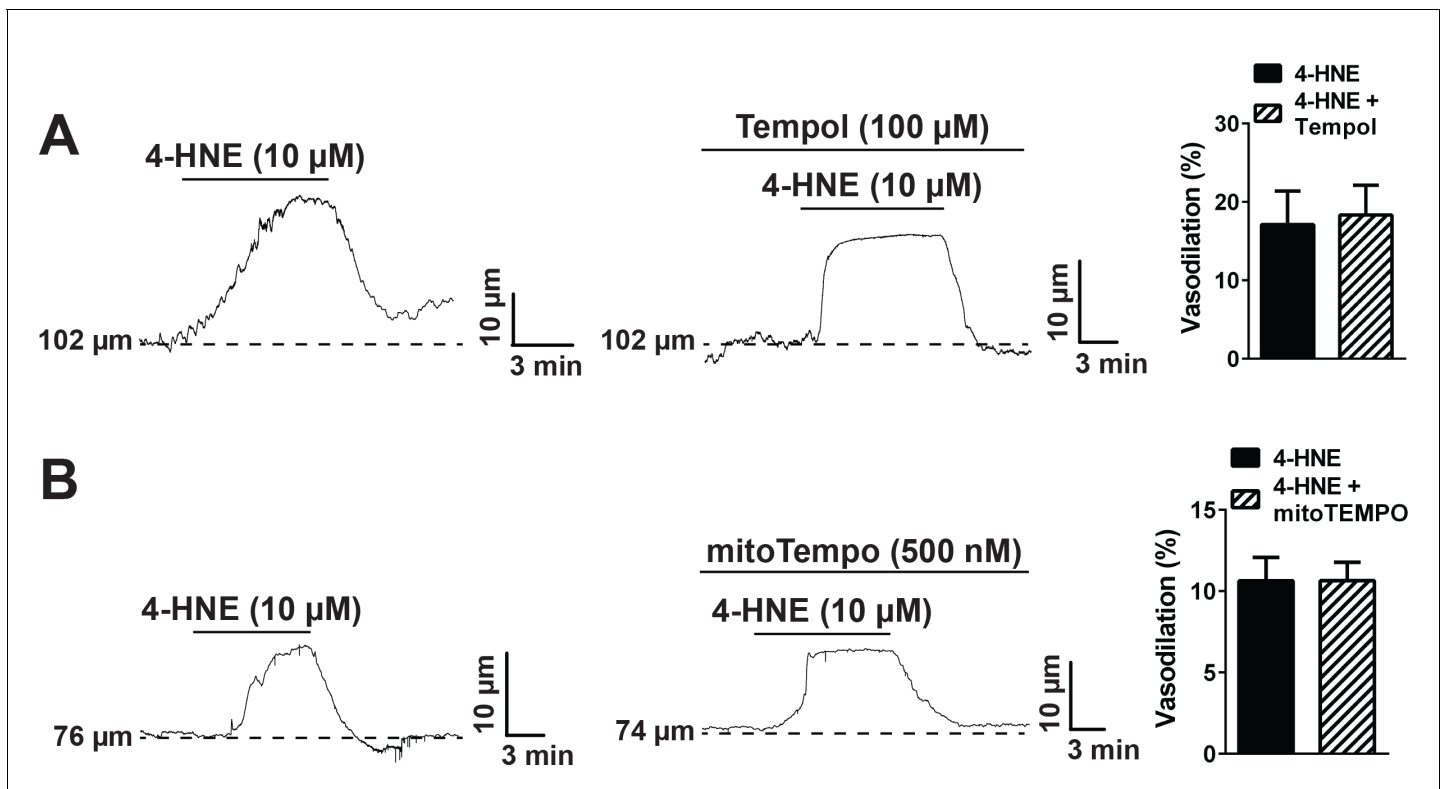


Figure 5—figure supplement 2. Superoxide dismutase mimetics do not directly inhibit TRPA1 channels. (A) The cell permeable superoxide dismutase (SOD) mimetic Tempol (100 μ M) did not alter dilation of pressurized cerebral arteries to the TRPA1 agonist 4-hydroxynonenal (4-HNE), as observed by the representative traces on the left and middle, and summary graph on the right. N = 3 arteries from three different mice. (B) Similarly, the mitochondria-targeted SOD mimetic mitoTEMPO (500 nM) did not affect TRPA1-mediated dilation caused by exposure to 4-HNE. N = 5 arteries from three different mice. Arteries used for pressure myography experiments were not incubated with EGTA-AM or CPA.

DOI: <https://doi.org/10.7554/eLife.35316.037>

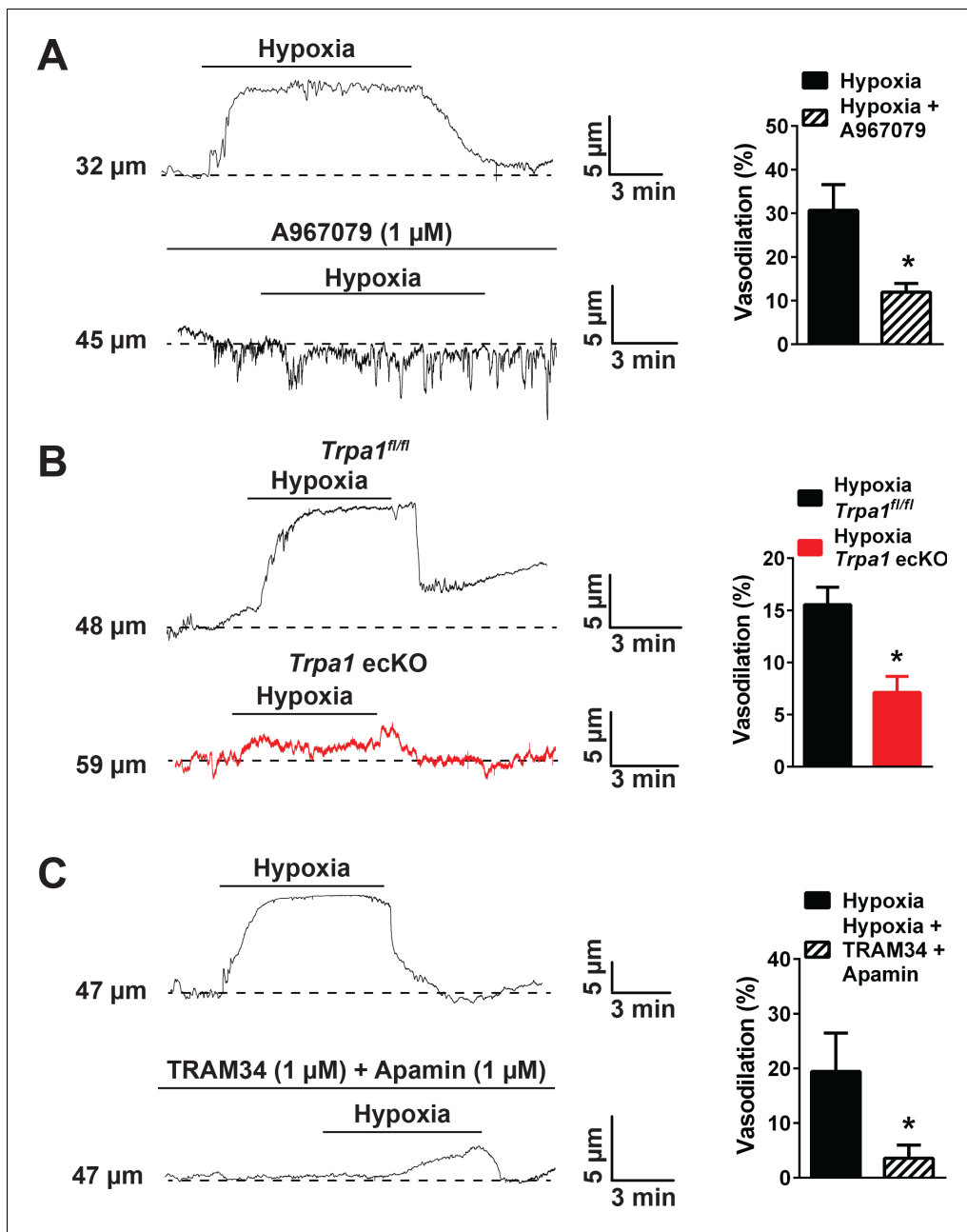


Figure 6. Hypoxia-induced cerebral artery dilation is dependent on endothelial TRPA1, $\text{K}_{\text{Ca}3.1}$ and $\text{K}_{\text{Ca}2.3}$ channels. (A) Representative traces of luminal diameter of pressurized cerebral pial arteries (left) and summary data (right) showing hypoxia-induced dilation in the presence and absence of the selective TRPA1 inhibitor A967079 (* $p < 0.05$, Student's t-test; $n = 5$ arteries from three different mice). (B) Representative traces of the luminal diameter of pressurized cerebral pial arteries (left) and summary data (right) showing hypoxia-induced dilation in *Trpa1* ecKO mice and wildtype littermates (*Trpa1^{fl/fl}*) (* $p < 0.05$, Student's t-test; $n = 7-6$ arteries from three different mice). (C) Representative traces of the luminal diameter of pressurized cerebral pial arteries (left) and summary data (right) showing hypoxia-induced dilation in the presence of selective inhibitors of $\text{K}_{\text{Ca}3.1}$ (TRAM34, 1 μM) and $\text{K}_{\text{Ca}2.3}$ channels (apamin, 1 μM) (* $p < 0.05$, Student's t-test; $n = 5$ arteries from three different mice). The arteries used for pressure myography experiments were not treated with EGTA-AM or CPA.

DOI: <https://doi.org/10.7554/eLife.35316.040>

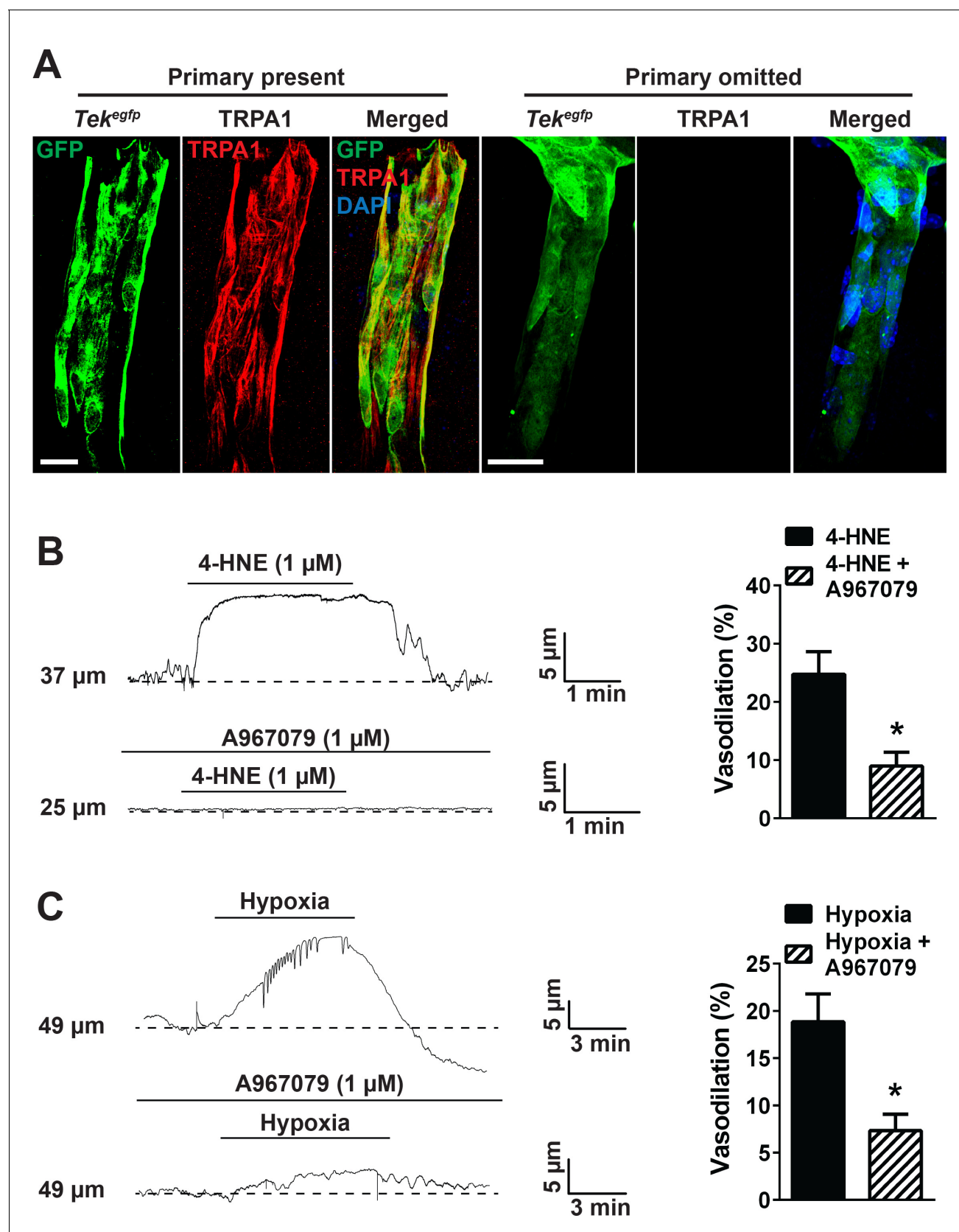


Figure 7. TRPA1 channel activity dilates cerebral penetrating arterioles. (A) Representative maximum intensity projection laser scanning confocal images showing immunolabeling of TRPA1 channels (red) in EGFP-expressing endothelial cells (green) of penetrating arterioles in the brain (left panels, Figure 7 continued on next page

Figure 7 continued

primary present). Scale bar = 20 μm . TRPA1 immunoreactivity was absent when the primary antibody was omitted (right panels). Nuclei of cells were stained by DAPI (blue). Scale bar = 20 μm . **(B)** Incubation of ex vivo pressurized penetrating arterioles with the TRPA1 agonist 4-HNE (1 μM) induced arteriolar dilation which was significantly diminished by A967079 (1 μM). Representative traces are shown on the left and the summary graph is shown on the right. (* $p < 0.05$, *Student's* t-test; $n = 5$ arteries from three different mice). **(C)** Hypoxia induced dilation of penetrating arterioles that was significantly blunted by A967079 (* $p < 0.05$, *Student's* t-test; $n = 6$ arteries from three different mice). The arterioles used for pressure myography experiments were not incubated with EGTA-AM or CPA.

DOI: <https://doi.org/10.7554/eLife.35316.042>

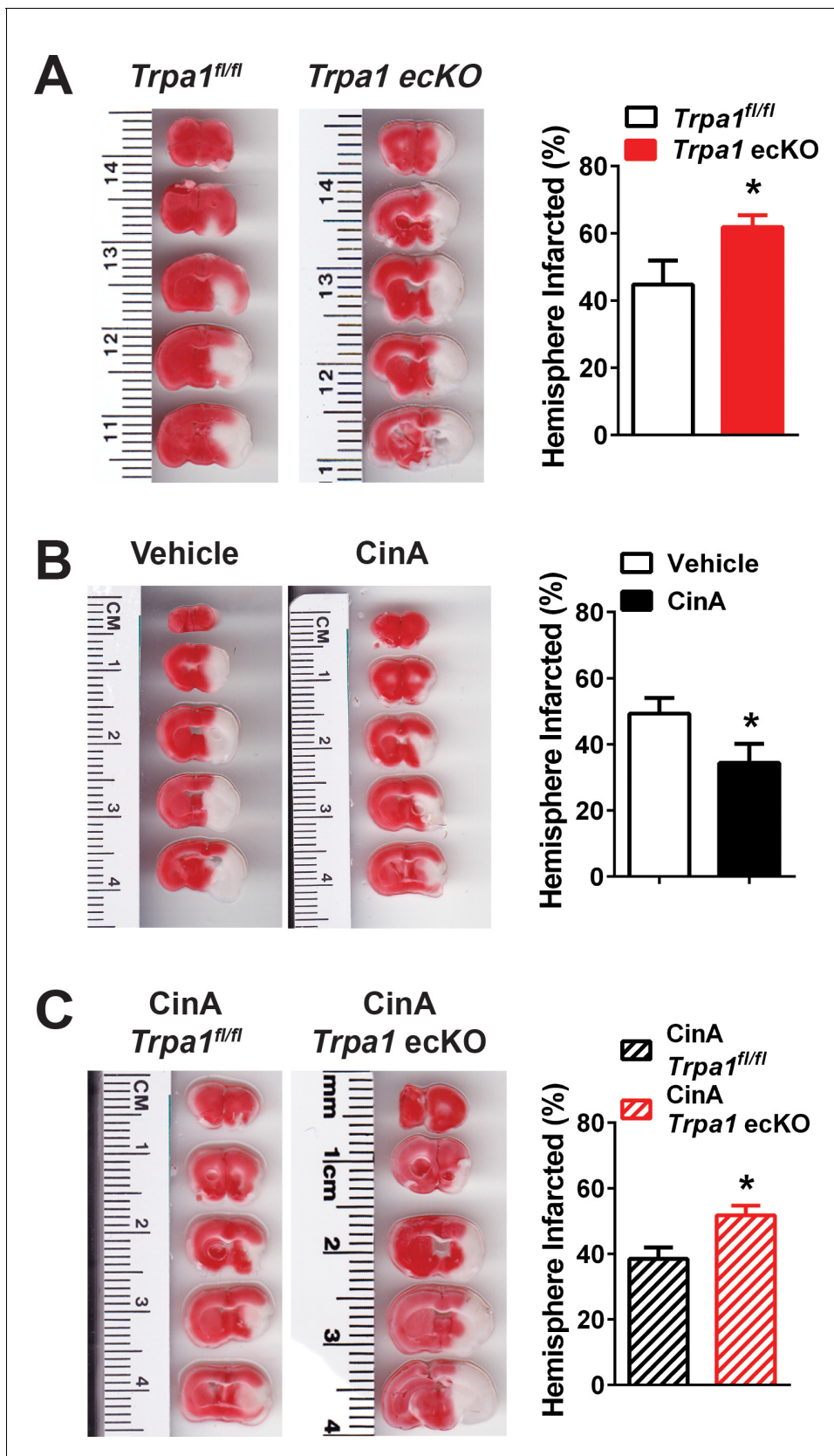


Figure 8. Endothelial cell TRPA1 channel activity protects against ischemic strokes. (A) Representative photographs of brain slices (left) and summary data (right) showing significantly greater ischemic damage 24 hr after MCAO in *Trpa1^{ecKO}* mice compared with *Trpa1^{fl/fl}*. Brain slices were stained

Figure 8 continued on next page

Figure 8 continued

with 2,3,5-triphenyltetrazolium chloride (TTC), which stains metabolically active tissue red, whereas infarcted tissue remains unstained (white). Infarcted areas were quantified and expressed as a percentage of total hemisphere area (* $p < 0.05$, *Student's t-test*; $n = 5$ –5 mice). (B) Representative photographs of brain slices (left) and summary data (right) showing reduced cerebral ischemic damage in wildtype C57/bl6 mice treated with the TRPA1 channel activator cinnamaldehyde (CinA, 50 mg/kg i.p.), injected 15 min after MCAO (* $p < 0.05$ for CinA vs. vehicle, *Student's t-test*; $n = 5$ –6 mice). (C) Representative photographs of brain slices (left) and summary data (right) showing that the protective effects of CinA were blunted in *Trpa1* eKO mice (* $p < 0.05$ for CinA-treated *Trpa1* eKO mice vs. CinA-treated *Trpa1*^{fl/fl} mice, *Student's t-test*; $n = 6$ –5 mice). Legends for Supplemental Figures.

DOI: <https://doi.org/10.7554/eLife.35316.044>

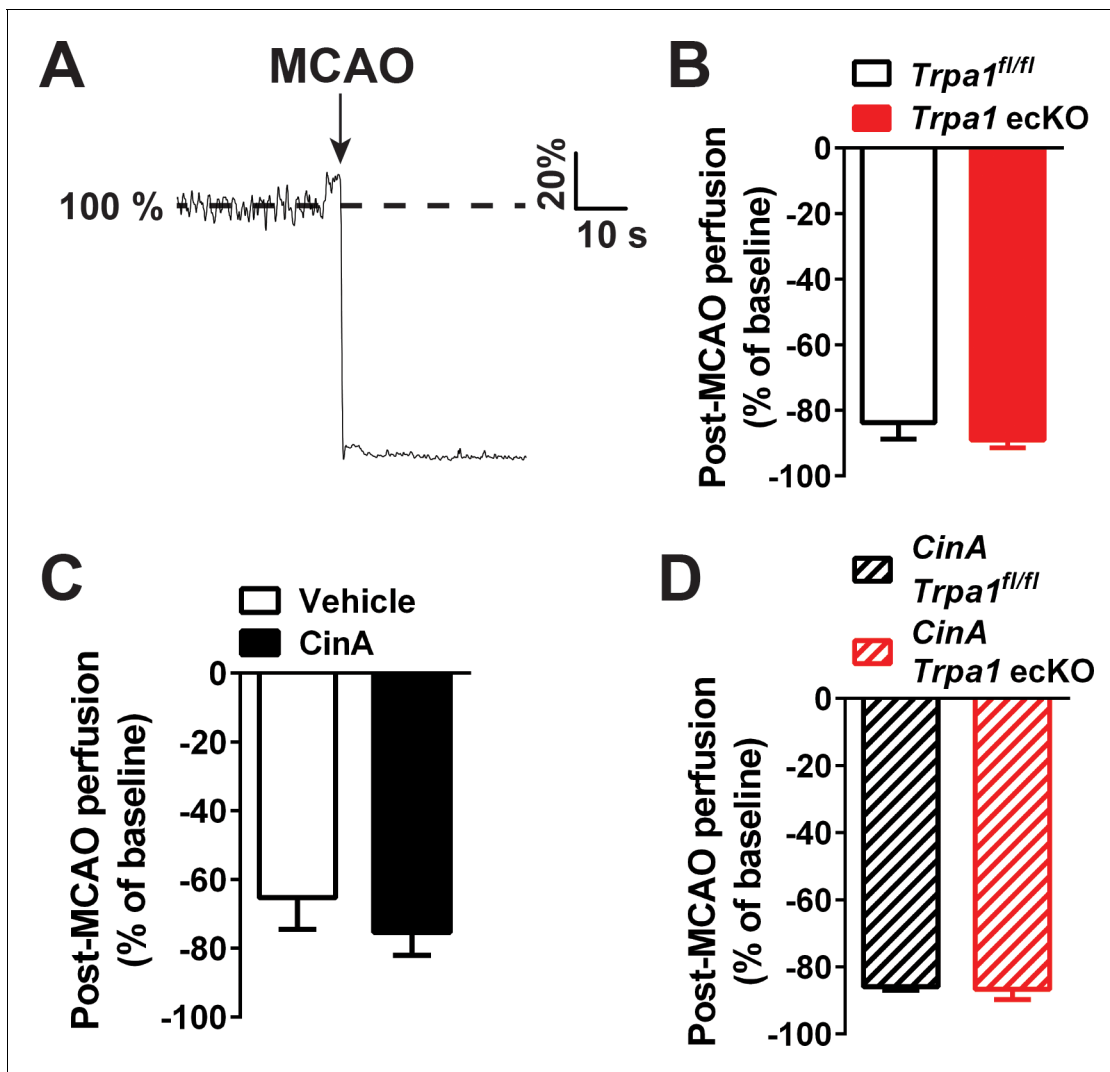


Figure 8—figure supplement 1. Post-MCAO perfusion is not significantly different between all experimental groups. (A) Representative laser Doppler flowmetry trace showing a sharp reduction in perfusion of the middle cerebral artery vascular territory after MCAO. Perfusion data are shown as a % of pre-occlusion perfusion. (B–D) Laser Doppler flowmetry assessment of cerebral perfusion to the middle cerebral artery territory showed that the extent of MCA occlusion was not significantly different between mice from all treatments and genetic backgrounds.

DOI: <https://doi.org/10.7554/eLife.35316.045>

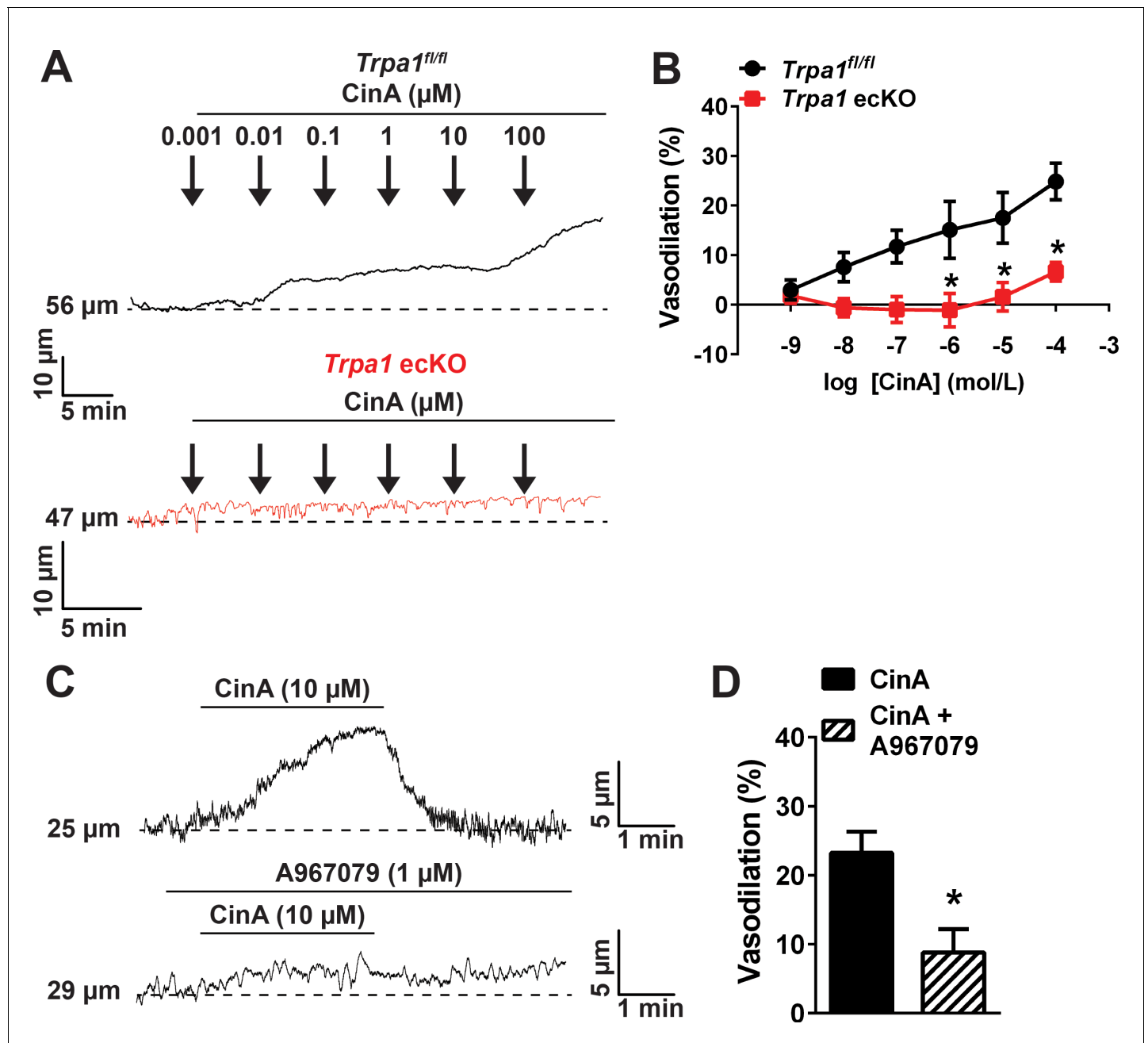


Figure 8—figure supplement 2. Cinnamaldehyde causes cerebral artery and arteriolar dilation by activating TRPA1 channels in endothelial cells. (A) Representative traces of the lumen diameter of pressurized cerebral arteries incubated with increasing concentrations of CinA (1 nM to 100 μM) in *Trpa1^{fl/fl}* (top trace, black) and *Trpa1 ecKO* mice (bottom trace, red). (B) Summary graph showing that CinA induces a concentration dependent dilation of cerebral arteries via TRPA1 channels located in endothelial cells. **p*<0.05, *n* = 6–6 arteries from three different *Trpa1^{fl/fl}* and three different *Trpa1 ecKO* mice. (C–D) CinA (30 μM) induces dilation of pressurized penetrating arterioles via TRPA1 channels, as evidenced by the representative traces (C) and the summary data (D). **p*<0.05, *n* = 5 arterioles from three different mice. Arteries and arterioles used for pressure myography experiments were not incubated with EGTA-AM or CPA.

DOI: <https://doi.org/10.7554/eLife.35316.047>

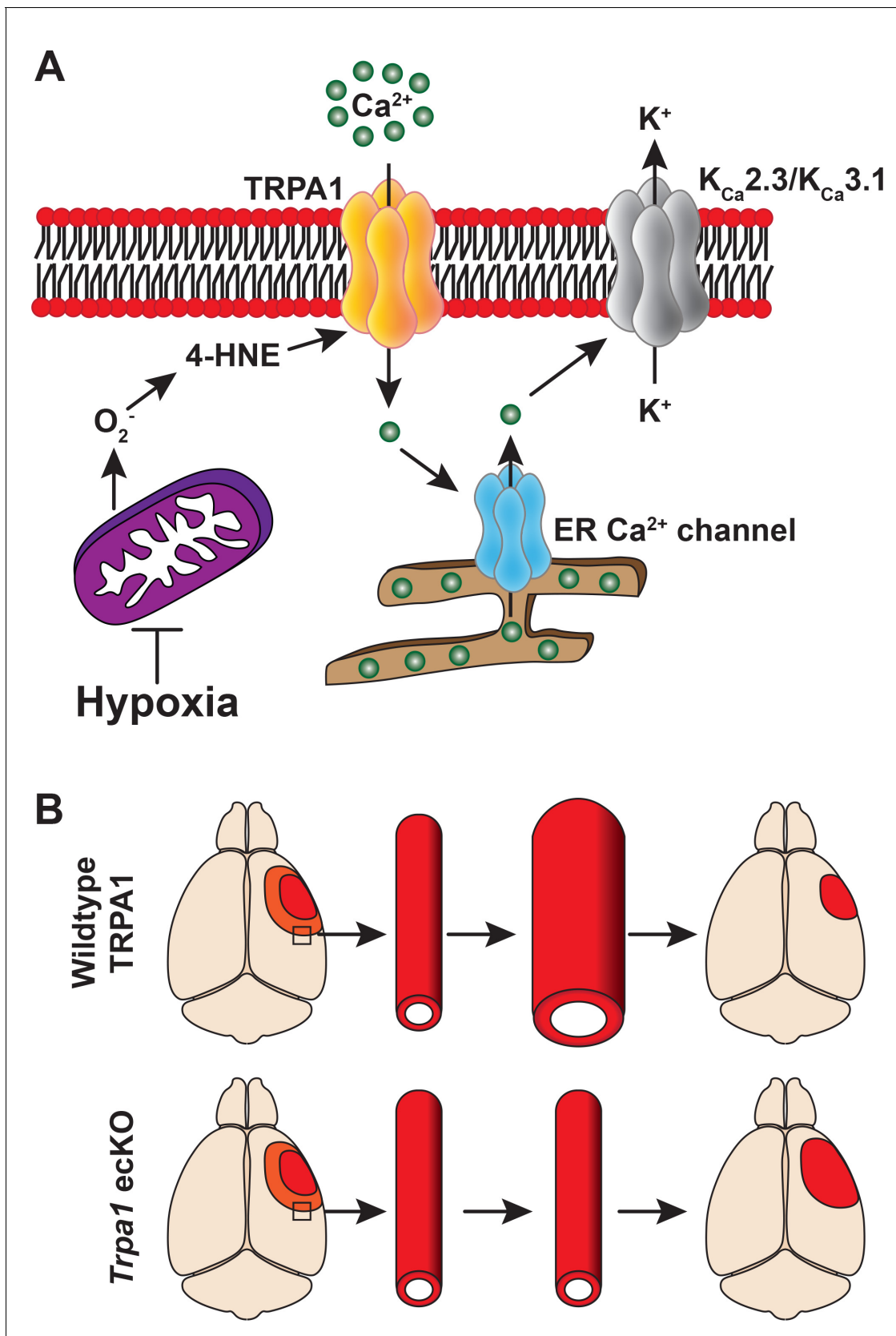


Figure 8—figure supplement 3. Mechanism of endothelial TRPA1 channel-mediated neuroprotection. (A) Acute hypoxia induces a mitochondria-dependent increase in superoxide production, which leads to accumulation of the lipid peroxide 4-hydroxynonenal (4-HNE) in endothelial cells. 4-HNE

Figure 8—figure supplement 3 continued on next page

Figure 8—figure supplement 3 continued

is an endogenous activator of the TRPA1 channel, increasing the frequency of Ca^{2+} influx events – TRPA1 sparklets, which is amplified by Ca^{2+} -induced Ca^{2+} -release from the endoplasmic reticulum. The subcellular increase in intracellular Ca^{2+} activates $\text{K}_{\text{Ca}2.3}$ and $\text{K}_{\text{Ca}3.1}$, resulting in K^{+} efflux and vasodilation. (B) In vivo, endothelial cell TRPA1 channel activity may act as an adaptive mechanism to prevent infarct expansion (red) by promoting vasodilation in the ischemic penumbra (orange). Endothelial-cell specific deletion of *Trpa1* removes this protection, ultimately leading to an increase in infarct volume following an ischemic stroke.

DOI: <https://doi.org/10.7554/eLife.35316.049>